







## RESEARCH ARTICLE

# Brain Dynamics Complexity as a Signature of Cognitive Decline in Parkinson's Disease

Eleonora Fiorenzato, PhD, PsyD,<sup>1</sup>  Sadaf Moaveninejad, PhD,<sup>2</sup>  Luca Weis, PhD,<sup>1,3</sup>   
 Roberta Biundo, PhD, PsyD,<sup>1,4,5</sup>  Angelo Antonini, MD, PhD,<sup>1,2,4</sup>  and Camillo Porcaro, PhD<sup>2,6,7\*</sup> 

<sup>1</sup>*Parkinson's Disease and Movement Disorders Unit, Department of Neuroscience, Centre for Rare Neurological Diseases (ERN-RND), University of Padova, Padova, Italy*

<sup>2</sup>*Department of Neuroscience and Padova Neuroscience Center, University of Padua, Padua, Italy*

<sup>3</sup>*IRCCS, San Camillo Hospital, Venice, Italy*

<sup>4</sup>*Department of Neuroscience, Center for Neurodegenerative Disease Research (CESNE), University of Padova, Padova, Italy*

<sup>5</sup>*Department of General Psychology, University of Padua, Padua, Italy*

<sup>6</sup>*Institute of Cognitive Sciences and Technologies-National Research Council, Rome, Italy*

<sup>7</sup>*Centre for Human Brain Health and School of Psychology, University of Birmingham, Birmingham, United Kingdom*

**ABSTRACT: Background:** Higuchi's fractal dimension (FD) captures brain dynamics complexity and may be a promising method to analyze resting-state functional magnetic resonance imaging (fMRI) data and detect the neuronal interaction complexity underlying Parkinson's disease (PD) cognitive decline.

**Objectives:** The aim was to compare FD with a more established index of spontaneous neural activity, the fractional amplitude of low-frequency fluctuations (fALFF), and identify through machine learning (ML) models which method could best distinguish across PD-cognitive states, ranging from normal cognition (PD-NC), mild cognitive impairment (PD-MCI) to dementia (PDD). Finally, the aim was to explore correlations between fALFF and FD with clinical and cognitive PD features.

**Methods:** Among 118 PD patients age-, sex-, and education matched with 35 healthy controls, 52 were classified with PD-NC, 46 with PD-MCI, and 20 with PDD based on an extensive cognitive and clinical evaluation. fALFF and FD metrics were computed on rs-fMRI data and used to train ML models.

**Results:** FD outperformed fALFF metrics in differentiating between PD-cognitive states, reaching an overall accuracy of 78% (vs. 62%). PD showed increased neuronal dynamics complexity within the sensorimotor network, central executive network (CEN), and default mode network (DMN), paralleled by a reduction in spontaneous neuronal activity within the CEN and DMN, whose increased complexity was strongly linked to the presence of dementia. Further, we found that some DMN critical hubs correlated with worse cognitive performance and disease severity.

**Conclusions:** Our study indicates that PD-cognitive decline is characterized by an altered spontaneous neuronal activity and increased temporal complexity, involving the CEN and DMN, possibly reflecting an increased segregation of these networks. Therefore, we propose FD as a prognostic biomarker of PD-cognitive decline. © 2023 The Authors. *Movement Disorders* published by Wiley Periodicals LLC on behalf of International Parkinson and Movement Disorder Society.

**Key Words:** Parkinson's disease; fractal dimension; mild cognitive impairment; dementia; neural networks

This is an open access article under the terms of the [Creative Commons Attribution-NonCommercial-NoDerivs](https://creativecommons.org/licenses/by-nc-nd/4.0/) License, which permits use and distribution in any medium, provided the original work is properly cited, the use is non-commercial and no modifications or adaptations are made.

\***Correspondence to:** Prof. Camillo Porcaro, Department of Neuroscience—DNS, University of Padua, Via Giustiniani, 5–35128 Padua, Italy; E-mail: [camillo.porcaro@unipd.it](mailto:camillo.porcaro@unipd.it)

**Relevant conflicts of interest/financial disclosures:** Nothing to report. Full financial disclosures and author roles are documented at the end of the manuscript.

**Funding agency:** none.

[Correction added on 20 December 2023, after first online publication: The affiliation order has been updated.]

**Received:** 26 July 2023; **Revised:** 13 November 2023; **Accepted:** 17 November 2023

**Published online 6 December 2023 in Wiley Online Library** ([wileyonlinelibrary.com](https://www.wileyonlinelibrary.com)). DOI: 10.1002/mds.29678

Parkinson’s disease (PD) is a clinical syndrome with variable clinical presentations, representing one of the fastest-growing neurodegenerative conditions.<sup>1</sup> Current therapeutic strategies can markedly improve motor disability but are only marginally beneficial to cognitive decline and dementia. For this reason, early identification of cognitive deficits and prevention of dementia is essential to slow disease progression and extend the patient’s daily functional independence.<sup>2</sup>

Resting-state functional magnetic resonance imaging (rs-fMRI) has been widely used to study brain activity and connectivity alterations in PD. Among the variety of resting-state approaches, the fractional amplitude of low-frequency fluctuation (fALFF) is a sensitive and reliable measure that can detect the spontaneous activity of brain neurons (0.01–0.1 Hz), including changes associated with mild cognitive impairments (MCI)<sup>3</sup> and motor severity in PD.<sup>4</sup>

Aligned with these observations, a meta-analysis of the most recent literature reported specific resting-state network (RSN) disruptions in PD with cognitive deficits, mostly involving the default mode network (DMN).<sup>5</sup> However, these findings rely on previously published studies with some critical methodological limitations: they were based on relatively small samples and did not include demented PD patients. To overcome these caveats, in a further study, we extended these results by applying a dynamic functional connectivity (FC) approach to rs-MRI data in a large cohort of PD patients.<sup>6</sup> We found that the presence of dementia was associated with increased segregation and reduced “crosstalk” between brain networks, confirming altered temporal properties in dynamic connectivity as a potential biomarker of PD-cognitive decline. However, it is worth mentioning that this method could not differentiate PD with mild cognitive impairment (PD-MCI) from PD with normal cognition (PD-NC).

Given the diverse range of cognitive impairments observed in PD and the intricate mechanisms underlying these deficits,<sup>7</sup> there is a growing interest in applying more sophisticated nonlinear methodologies to characterize the dynamics of brain neural activity. These advanced techniques offer the potential for more precise and comprehensive extraction of signal information. Notably, nonlinear methods have been proposed as better suited for capturing the complexity of the blood oxygen level-dependent (BOLD) signal due to its irregular and non-periodic hemodynamic fluctuations.<sup>8</sup> In contrast, linear methods, such as the well-known fast Fourier transformation, make an assumption of the brain signal’s stationarity, which may not hold true for electrophysiological and neuroimaging data, often exhibiting irregular and nonperiodic patterns in both healthy and neurological states. Modern nonlinear approaches, such as the fractal dimension (FD), have gained recognition as more effective metrics for analyzing and characterizing the intricate nature of brain signals. One key advantage of

FD is its independence from the inherent nature of the signal, whether it be stationary, nonstationary, deterministic, or stochastic. For a comprehensive review on this subject, refer to Kesić and Spasić.<sup>9</sup>

The concept of FD originates from chaos theory and is based on the idea that a simple process, when repeated endlessly, can result in a highly complex process, forming the foundation of fractal theory.<sup>9</sup> These intricate interactions within the brain’s activity generate patterns that exhibit self-similarity across various temporal and spatial scales. That is, neural activity exhibits similar features repeatedly in a scale-free manner. The strength of FD lies in its ability to detect potentially “hidden information” that may have been previously overlooked in neurophysiological time-series data, spanning various levels of analysis, from neuronal spiking activity to electroencephalogram (EEG), fMRI, electromyography signals,<sup>10</sup> and even structural MRI data.<sup>11</sup>

This nonlinear method has been proposed as a useful indicator of several neurological conditions, such as early Alzheimer’s disease (AD),<sup>12,13</sup> multiple sclerosis,<sup>14</sup> frontotemporal dementia,<sup>15</sup> acute stroke,<sup>16</sup> migraine,<sup>17-19</sup> consciousness,<sup>19,20</sup> and genetic disorders.<sup>21</sup> Therefore, fractal analysis may better characterize the whole-brain dynamic alterations associated with PD-cognitive decline, compared to the more standard fMRI analysis techniques, because it allows us to detect the complexity of neuronal interactions underlying cognitive deficits.

Building on these observations, the aims of this work are as follows: The first aim was to explore the potential differences in intrinsic spontaneous brain activity, using a fALFF approach, in a large cohort of PD patients with an adequate representation across the entire cognitive spectrum, ranging from NC to dementia, as well as to compare PD with healthy control (HC) subjects. The second aim was to analyze the complexity of brain dynamics using a novel nonlinear method—the Higuchi’s FD—in PD patients versus HCs, as well as across PD-cognitive subgroups. The third aim was to compare FD results with the more established fALFF metric to identify using machine learning (ML) which method could best distinguish across cognitive states (PD-NC, PD-MCI, and dementia) and possibly predict cognitive decline in PD. Finally, we also explored correlations between fALFF and FD metrics with clinical and cognitive PD features.

## Patients and Methods

### Participants and Clinical Assessment

This is a cohort of 118 patients with PD and 35 HCs, which we have already described in a previous work.<sup>6</sup> Participants were recruited at the Parkinson Disease and Movement Disorders Unit, Neurology Clinic in Padua, and at the San Camillo Hospital, Venice. PD was diagnosed according to the clinical diagnostic criteria,<sup>22</sup> and

HCs were age-, gender- and education matched to patients. The Movement Disorder Society Unified Parkinson's Disease Rating Scale (MDS-UPDRS-III) and Hoehn and Yahr (HY) scale were adopted to assess disease severity, and the levodopa (L-dopa) and the dopamine agonist equivalent daily dosages were calculated for each patient.<sup>23</sup>

All subjects underwent a comprehensive neuropsychological battery (level II criteria of the MDS guidelines) as previously described,<sup>24</sup> specifically designed to target PD-cognitive deficits, which allow us to classify patients as PD-NC, PD-MCI, or PD with dementia (PDD) (for further details refer to the Supporting Information). The present study was approved by the Venice Research Ethics Committee, Venice, Italy. Written informed consent was obtained from all participants, and the research was completed in accordance with the Helsinki Declaration.

### MRI Acquisition, Preprocessing, and Functional MRI Data Analysis

Structural 3D T1-weighted and resting-state data were acquired using a Philips Achieva 1.5-T scanner (Philips Medical Systems, Amsterdam, Netherlands) with an eight-channel head coil. For further details, refer to the Supporting Information and for fMRI analyses to our previous study.<sup>6</sup> This process resulted in 35 meaningful independent components (ICs), which were classified into seven RSNs: basal ganglia, auditory (AN), visual, sensorimotor (SMN), cognitive executive (CEN), DMN, and cerebellar (CB) networks, as shown in Figure 1A and Table S1. Of note, as described in our previous work,<sup>6</sup> the time courses of 35 ICs underwent additional postprocessing to remove the remaining physiological and scanner noise. As shown by Allen et al,<sup>25</sup> time courses were detrended (linear, quadratic, and cubic trends), despiked using AFNI's 3dDespike algorithm, and then filtered using a fifth-order Butterworth low-pass filter with a 0.15-Hz high-frequency cutoff, and finally we regressed out the movement parameters.

### Fractional Amplitude of Low-Frequency Fluctuations

The linear measure, fALFF, was computed using Group ICA of fMRI Toolbox (GIFT, <https://trendscenter.org/software/gift/>), and the obtained results were compared to the nonlinear FD. The fALFF activity represents the relative contribution of low-frequency fluctuations within a specific frequency band (0.01–0.1 Hz) to the whole detectable frequency range.<sup>17,26</sup>

### Higuchi's FD

The characterization of BOLD signal RSNs using FD was extensively described in our previous works,<sup>8,17,27</sup> where all the formulas for its

calculation are reported. Briefly, a fractal is a shape that retains its structural detail despite a scaling factor. For this reason, complex objects can be described using FD.<sup>9,28,29</sup> FD is a highly sensitive measure to detect hidden information contained in physiological time series.<sup>9,30</sup> Although many approaches for FD computation have been reported, the Higuchi's method is the most widely accepted and accurate.<sup>31–33</sup> Here, we computed the Higuchi's FD, as described in the Supporting Information.

### PD-Cognitive State Prediction: An ML Approach

The data model preprocessing included age, fALFF, and FD values (of the 35 ICs), as relevant variables in further steps. The cognitive states (PD-NC/PD-MCI/PDD) were considered as ordinal target variables. Because the PD subgroups were imbalanced, after preprocessing and during the training phase of ML, the synthetic minority oversampling technique was adopted to resample the small subgroup obtaining a comparable numerosity and avoiding misclassifications.

### Features Engineering

Further, a derived multivariate measure, the pairwise distance (Pdist) between ICs, was computed using Mahalanobis metric. This calculation was performed twice: once for the fALFF values over 35 ICs and once for the FD values over 35 ICs. The resulting output in each case is an upper triangular matrix consisting of 595 total measures, calculated as  $[(35 \times 35) - 35]/2$ , which considers the symmetric nature of the matrix and excludes diagonal elements. To compute these distances, the Pdist function from the *scipy.spatial.distance* library in Python was adopted, setting the metric parameter to Mahalanobis. Using the Pdist metric would incorporate the covariance structure of the FD/fALFF values into the distance calculation, providing a more comprehensive measure of dissimilarity between ICs. These dissimilarity measures were adopted given their lower sensitivity over correlation metrics to movement artifacts<sup>34</sup> and a more robust estimate of FC.<sup>35,36</sup>

### Features Scaling

To ensure the fairness and effectiveness of ML models, it is necessary to preprocess the features by applying a scaling function to normalize them within a specific range. This preliminary step is crucial to avoid a disproportionate influence of certain features, due to their higher values rather than contributing to the model with their actual importance. Several scaling methods, including standard scaling, min–max scaling, and robust scaling, were evaluated and compared. Among these methods, the Standard Scaler showed the

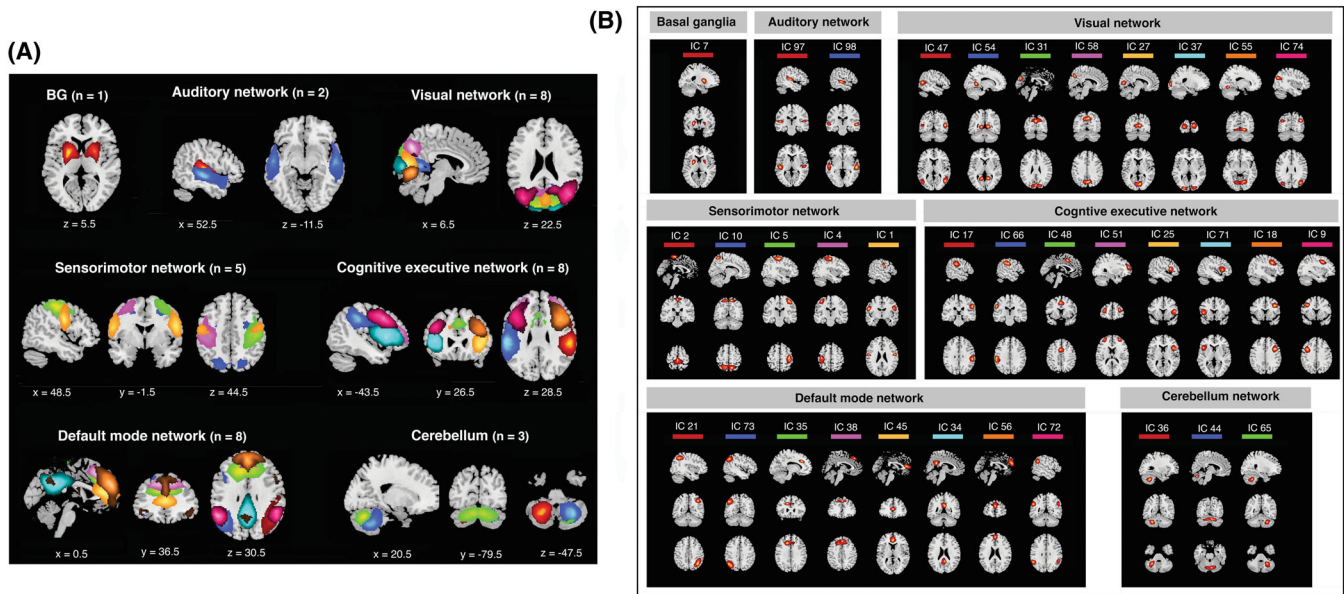


**FIG. 1.** Seven functional networks and 35 independent components (IC): **(A)** ICs ( $n = 35$ ) identified by group IC analysis. IC spatial maps divided on seven functional networks (basal ganglia [BG], AN [auditory network], VIS [visual network], SMN [sensorimotor network], CEN [central executive network], DMN [default mode network], and CB [cerebellar network]) based on their anatomical and functional properties. **(B)** Spatial maps for the 35 ICs. Spatial maps were thresholded with  $t > \mu + 4\sigma$ ,  $k > 100$ . Adapted from Fiorenzato et al.<sup>6</sup> [Color figure can be viewed at [wileyonlinelibrary.com](https://onlinelibrary.wiley.com)]

highest accuracy when applied to the input of the classifiers and selected for feature scaling.

### Features Ranking

To enhance the classification process, an optimization approach was employed to select informative features from the 595 pairwise distances and separately run for the FD and fALFF values. The feature selection process followed this procedure, as previously described.<sup>37</sup> The features were first ranked based on their one-way analysis of variance (ANOVA)  $F$ -values using the Python function `F-classif` from Python Scikit-learn library. This initial step is independent of features classification.<sup>38</sup> Then, features were arranged in descending order based on their scores. The 595 groups of pairwise distance vectors were created as follows: the first group consisted only of the highest-ranked feature, the second one included the two highest-ranked features, and the last group encompassed all the pairwise distances. The second step of the feature selection was integrated with the classification one; that is, the best classifier and features were simultaneously identified from the classification outcome, as detailed in the next paragraph. Each group was then individually provided as input to various ML models. The group that yielded the highest performance among the models was selected as the best features vector for further analyses. The highest-performing models identified the optimized features, which were the most relevant and discriminative among the initial pairwise distances set.

### Classification

Different ML algorithms were tested for their efficiency to discriminate between PD-cognitive states, after accurately tuning their hyperparameters. The examined algorithms included neural network (NN), support vector machine (SVM), random forest (RF), GradientBoost, K-nearest neighbors, and different combinations of these models through soft-voting and hard-voting. For each model, four accuracy measures were calculated as follows (TP, true positive; FP, false positive; FN, false negative; TN, true negative):  $\text{precision} = \text{TP}/(\text{TP} + \text{FP})$ ;  $\text{recall} = \text{TP}/(\text{TP} + \text{FN})$ ;  $\text{F1 score} = (2 \times \text{precision} \times \text{recall})/(\text{precision} + \text{recall})$  focused on positive class detection;  $\text{accuracy} = (\text{TP} + \text{TN})/(\text{TP} + \text{FP} + \text{TN} + \text{FN})$  in terms of positive and negative correctly classified observations. An accuracy threshold of 0.7 was considered moderate. The models were rigorously tested using a fivefold stratified cross-validation strategy, ensuring reliability and generalizability. This approach involved multiple iterations with diverse training and testing subsets, minimizing biases and inconsistencies in performance estimates. This strategy was repeated 10 times for thoroughness and reliability.

### Statistical Analysis

Demographic and cognitive data of HCs versus PD patients were compared using independent samples  $t$  test, whereas PD subgroups were compared across cognitive states (PD-NC/PD-MCI/PDD) using ANOVA models. Pearson's  $\chi^2$  test was used to compare categorical variables.

fALFF and FD average values, for the PD and HC groups, were obtained for each of the 35 ICs and  $z$ -transformed to allow their comparison. Similar to our previous work,<sup>6</sup>  $z$ -values were then residualized with nuisance variables (ie, age and gender).<sup>39</sup> Further, given that fALFF and FD measures were not normally distributed, despite the natural logarithm transformation, nonparametric statistics were adopted.

Mann-Whitney  $U$  test was run to compare the fALFF and FD signals of the seven RSNs between the HC and PD groups. To verify whether these differences were associated to PD-cognitive decline, nonparametric ANOVA, Kruskal-Wallis  $H$  test, was adopted to compare PD subgroups (PD-NC, PD-MCI vs. PDD) at the IC level within the significant RSNs that resulted as significant. Post hoc Dwass-Steel-Critchlow-Fligner test was adopted followed by multiple comparison corrections.

Spearman's correlation analyses were run between fALFF and FD metrics (in the altered ICs) and the PD clinical variables (eg, disease duration and motor severity) and cognition (Mini-Mental State Examination, Montreal Cognitive Assessment [MoCA], and cognitive performance in each domain), followed by multiple comparison corrections. The statistical significance threshold was set at  $P \leq 0.05$ ; the false discovery rate (FDR) was adopted to correct for multiple comparisons.

## Results

### Demographic, Clinical, and Cognitive Characteristics

HCs and PD patients (as whole group) were age-, gender-, and education matched (Table 1), but some differences in clinical characteristics between HCs and PD-MCI and PDD, as well as between PD subgroups, were observed (Table 1). Twenty PD patients (16.9%) fulfilled the criteria of dementia, 46 of PD-MCI (39.0%), and the remaining 52 (44.1%) of PD-NC. The neuropsychological differences between the HC and PD subgroups are presented in Tables S2 and S3.

### Independent Components and RSNs

As shown in Figure 1B, all the 35 IC spatial maps were determined and classified into seven RSNs based on their anatomical and functional properties. More details of the IC spatial maps are presented in Table S1.

### fALFF and FD Differences: HC versus PD, and between PD Subgroups

#### fALFF Results

Compared to HCs, PD patients showed reduced fALFF values in the DMN ( $U = 1028.00$ ,  $z = -4.504$ ,  $P < 0.001$ ) and CEN ( $U = 1352.00$ ,  $z = -3.097$ ,  $P = 0.002$ ), whereas a significant increase was observed in

the AN ( $U = 1465.00$ ,  $z = -2.606$ ,  $P = 0.009$ ) (see Fig. 2A; Fig. S1).

Further exploring these significant RSNs—AN, DMN, and CEN—we investigated differences between PD-cognitive subgroups. In the AN, we found a significant difference in IC97 ( $H(2) = 8.80$ ,  $P = 0.012$ ), with PDD showing lower fALFF than PD-NC ( $W = -4.00$ ,  $P = 0.013$ ) (Fig. 2B; Fig. S2A). Similarly, in the CEN, we found significant differences between PD subgroups, involving IC17 and IC25 ( $H(2) = 11.28$ ,  $P = 0.004$ ;  $H(2) = 6.58$ ,  $P = 0.04$ , respectively). In both these ICs, PDD showed a reduced fALFF activity than PD-NC ( $W = -4.80$ ,  $P = 0.002$  and  $W = -3.45$ ,  $P = 0.039$ , respectively) (Fig. 2B; Fig. S2A), whereas there was no difference between PDD and PD-MCI subgroups following multiple comparison corrections: IC17 ( $W = -2.80$ ,  $P = 0.117$ ) and IC25 ( $W = -3.02$ ,  $P = 0.083$ ). In the DMN, fALFF activity did not differ between PD subgroups, and overall, no differences were observed between PD-NC and PD-MCI.

### Fractal Dimension Results

PD showed higher FD values in the SMN ( $U = 1232.00$ ,  $z = -3.61$ ,  $P < 0.001$ ), CEN ( $U = 1569.00$ ,  $z = -2.15$ ,  $P = 0.031$ ), and DMN ( $U = 1389.00$ ,  $z = -2.94$ ,  $P = 0.003$ ) compared to HC (Fig. 2C; Fig. S3).

Differences within the CEN were found in IC48 ( $H(2) = 7.80$ ,  $P = 0.020$ ), with PDD showing statistically significantly increased FD values than PD-NC ( $W = 3.67$ ,  $P = 0.026$ ) and PD-MCI ( $W = 3.59$ ,  $P = 0.030$ ) (Fig. 2D; Fig. S2B). In the DMN, the differences were regarding IC45 ( $H(2) = 6.35$ ,  $P = 0.042$ ) and IC34 ( $H(2) = 8.80$ ,  $P = 0.024$ ). In IC45, PDD showed higher FD values than PD-NC ( $W = 3.33$ ,  $P = 0.049$ ), whereas compared to PD-MCI there was only a trend, after multiple comparison correction ( $W = 3.22$ ,  $P = 0.060$ ). In IC34, PDD presented a higher FD than PD-NC and PD-MCI ( $W = 3.77$ ,  $P = 0.021$  and  $W = 3.32$ ,  $P = 0.050$ , respectively). In the SMN, there were no differences between PD subgroups.

### Correlations of fALFF and FD Measures with PD Clinical Features

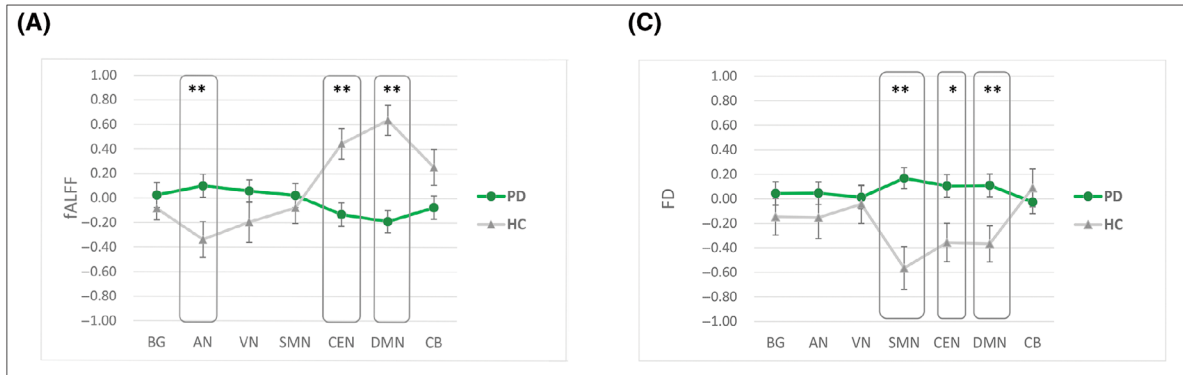
Regarding fALFF metric, IC97, as part of the AN, negatively correlated with motor severity (MDS-UPDRS-III) ( $r_s = -0.25$ ,  $pFDR = 0.039$ ) and positively correlated with global cognition (MoCA) ( $r_s = 0.30$ ,  $pFDR = 0.010$ ), attention/working memory ( $r_s = 0.25$ ,  $pFDR = 0.031$ ), and language abilities ( $r_s = 0.23$ ,  $pFDR = 0.035$ ) (Table S4). This means that a reduction in fALFF activity in the AN (mostly involving the bilateral superior temporal gyrus) was linked to greater motor severity, poorer

**TABLE 1** Demographic and clinical data of HC and PD as well as PD subgroups

	HC (n = 35)		PD (n = 118)		PD subgroups				HC vs. PD		P-value	
	Mean (SD)		Min-max		PD-NC (n = 52)		PD-MCI (n = 46)		PDD (n = 20)			HC vs. PD
	Mean (SD)	Min-max	Mean (SD)	Min-max	Mean (SD)	Min-max	Mean (SD)	Min-max	Mean (SD)	Min-max		PD-MCI vs. PDD
Age	61.29 (8.98)	45-83	63.68 (11)	34-85	58.63 (9.58)	34-85	65.87 (11.37)	36-81	71.75 (6.62)	55-82	0.241	<0.001
Education	12.43 (4.02)	5-18	10.76 (4.52)	2-18	12.67 (3.86)	5-18	9.61 (4.49)	2-18	8.45 (4.36)	3-18	0.082	0.018
Sex (m/f)	18/17		79/39								0.094	
Disease duration (y)	-	-	9.81 (5.33)	1-28	9.48 (4.62)	1-20	9.09 (5.4)	2-28	12.35 (6.35)	4-23		
Age of onset	-	-	53.8 (12.06)	13-78	49.19 (9.45)	29-73	56.57 (13.54)	13-75	59.4 (10.58)	40-78		0.003
MDS-UPDRS-III	-	-	23.49 (14.53)	4-77	16.41 (8.53)	4-41	26.82 (15.04)	7-68	35.6 (16.71)	12-77		<0.001
LEDD	-	-	887.83 (512.6)	0-2296	859.23 (553.97)	0-2080	947.92 (485.81)	60-2296	824.15 (472.84)	150-1955		
DAED	-	-	136.17 (113.82)	0-480	160.19 (113.19)	0-480	143.24 (112.23)	0-390	60 (88.74)	0-240		0.003
Cognitive features												
MMSE	29.03 (1.38)	23-30	26.97 (3.05)	17-30	28.87 (1.07)	26-30	26.83 (2.32)	20-30	22.4 (3.07)	17-27	<0.001	<0.001
MoCA	25.86 (2.58)	19-30	22.08 (5.05)	9-30	25.62 (2.15)	21-30	21.11 (4.21)	11-29	15.15 (3.98)	9-22	<0.001	<0.001

Note: Two-sample *t* test was used to compare between-group differences (HC vs. PD), whereas one-way analysis of variance was used for the comparisons between subgroups (HC, PD-NC, PD-MCI, and PDD).  $\chi^2$  test was used for the categorical variable. Multiple comparison correction was applied. No differences between HC and PD-NC were noted. Adapted from Fiorenzato et al.<sup>6</sup>  
 Abbreviations: HC, healthy controls; PD, Parkinson's disease; PD-NC, PD with normal cognition; PD-MCI, PD with mild cognitive impairment; PDD, PD with dementia; SD, standard deviation; MDS-UPDRS, Movement Disorder Society Unified Parkinson's Disease Rating Scale; LEDD, levodopa equivalent daily dose; DAED, dopamine agonist equivalent dose; MMSE, Mini-Mental State Examination; MoCA, Montreal Cognitive Assessment.

PD vs. HCs



PD-NC, PD-MCI vs. PDD

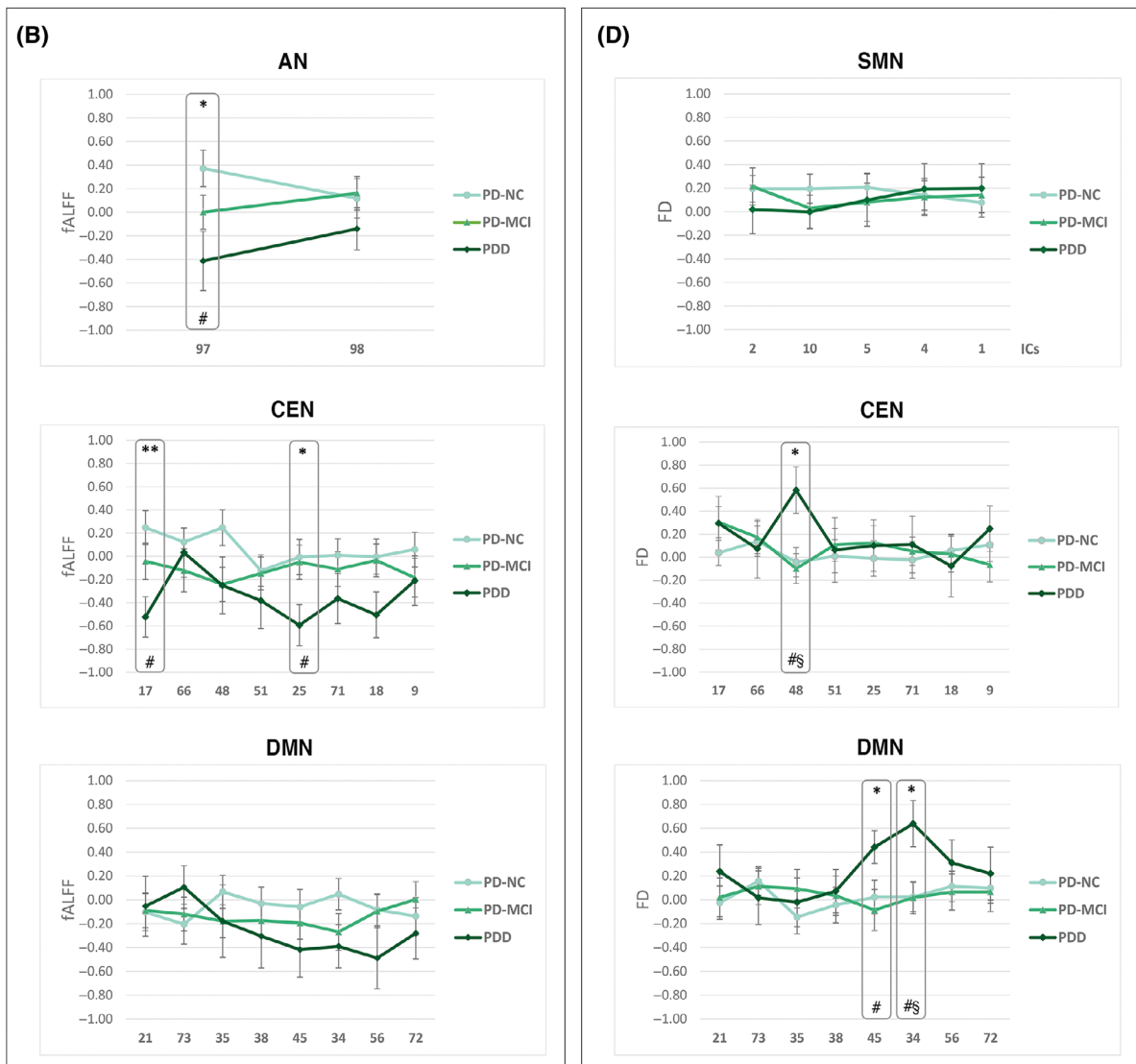


**FIG. 2.** fALFF (fractional amplitude of low-frequency fluctuation) and FD (fractal dimension) between-group comparisons. Differences between PD (Parkinson’s disease) and HC (healthy controls) in (A) fALFF activity and (C) FD in the seven RSNs (resting-state network). Differences across PD subgroups in (B) fALFF activity and (D) FD within the statistically significant ICs (independent component). Mean  $\pm$  standard deviation are displayed. \* $P \leq 0.05$ , \*\* $P \leq 0.01$ . Significant post hoc results after multiple comparison correction: #PDD (PD with dementia) versus PD-NC (PD with normal cognition); §PDD versus PD-MCI (PD with mild cognitive impairment). [Color figure can be viewed at [wileyonlinelibrary.com](http://wileyonlinelibrary.com)]

global cognitive performance, and worse attentive and language abilities.

For FD values, IC45, as part of the DMN, positively correlated with disease severity (HY score) ( $r_s = 0.27$ ,  $pFDR = 0.032$ ), whereas a negative correlation was observed with memory functions ( $r_s = -0.24$ ,  $pFDR = 0.043$ ). These findings suggest that higher FD values in the DMN, involving the anterior cingulate cortex (ACC), were associated with a greater disease severity and poorer memory abilities.

### fALFF and FD IC Pairwise Difference across PD Cognitive Spectrum

We found that fALFF activity presented a pattern characterized by higher dissimilarity between IC pairs, with PDD showing reduced fALFF differences between IC pairs than PD-NC and PD-MCI (Fig. 3A). Of note,

fALFF differences between IC pairs were widespread throughout the whole brain, involving the majority of ICs and related RSNs.

Regarding FD measures across all PD-cognitive states, we observed that IC pairs were more similar between each other, presenting a similar level of complexity. Of note, this similarity pattern between IC pairs was increasing with cognitive severity (PD-NC > PD-MCI > PDD) (see Fig. 3A; Fig. S4)—the more severe the level of cognitive decline, more similar were the IC pairs in terms of complexity. Our results highlighted that particularly within the PDD group, the ICs were more similar in their complexity level, than PD-NC and PD-MCI.

### PD-Cognitive States Prediction

IC similarities in terms of fALFF and FD, as operationalized by pairwise Mahalanobis distances

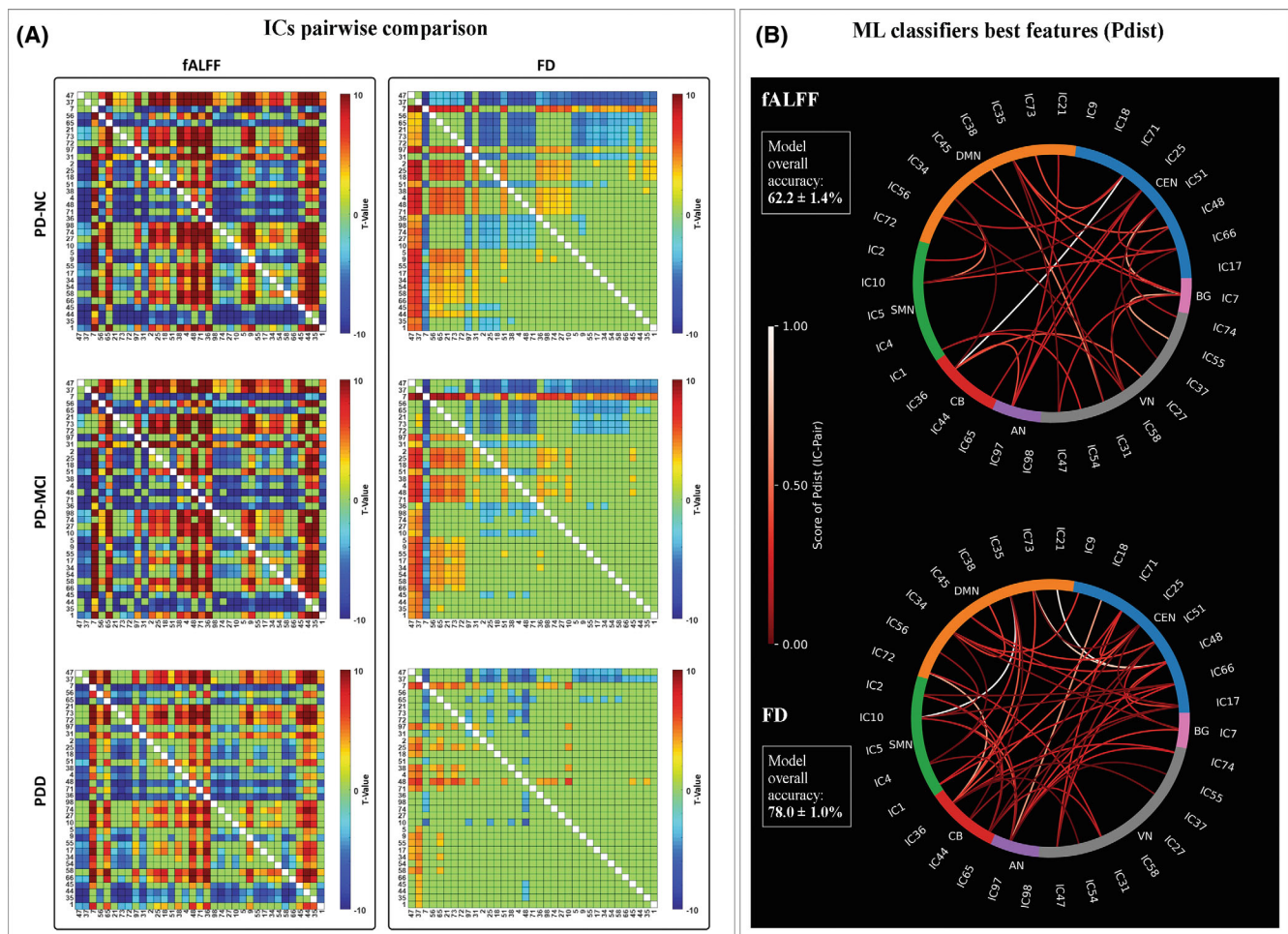


**FIG. 3.** IC (independent component) pairwise comparisons and machine learning best predictors for fALFF (fractional amplitude of low-frequency fluctuation) and FD (fractal dimension) metrics. **(A)** Nonparametric permutation *t* test (10,000 permutations) between IC pairs to test the difference between IC pairs, across the entire PD-cognitive spectrum (PD-NC [PD with normal cognition], PD-MCI [PD with mild cognitive impairment], and PDD [PD with dementia]). For visual purposes, not significant results after false discovery rate (FDR) correction ( $P < 0.01$ ) were classified as zero (Nichols, T.E., & Holmes, A.P. (2002). Hum Brain Mapp, 15 (1):1–25); **(B)** Mahalanobis distances (Pdlist) of all pairs (for fALFF and FD) that were more relevant for the machine learning models to distinguish between PD-cognitive states. For brevity, white color of the lines indicates a stronger similarity between IC pairs and thus their higher relevance within ML models, and red lines indicate a lower relevance. The intensity of the color indicates the strength of the similarity. Basal ganglia (BG), auditory (AN), sensorimotor (SMN), visual (VIS), cognitive executive (CEN), default mode (DMN), and cerebellar (CB) networks; ML, machine learning. [Color figure can be viewed at [wileyonlinelibrary.com](http://wileyonlinelibrary.com)]



**TABLE 2** Classification accuracy based on pairwise Mahalanobis distances between the ICs from seven RSNs

		Precision	Recall	F1 score	Support
fALFF	PD-NC	0.64	0.72	0.68	50
	PD-MCI	0.62	0.56	0.59	45
	PDD	0.67	0.63	0.65	19
	Macro average	0.64	0.64	0.64	114
	Weighted average	0.64	0.64	0.64	114
	Overall accuracy				62.2 ± 1.4%
		Precision	Recall	F1 score	Support
FD	PD-NC	0.81	0.86	0.83	50
	PD-MCI	0.78	0.78	0.78	45
	PDD	0.81	0.68	0.74	19
	Macro average	0.80	0.77	0.79	114
	Weighted average	0.80	0.80	0.80	114
	Overall accuracy				78.0 ± 1.0%

Note: Machine learning classification models utilizing pairwise Mahalanobis distance measures for ICs from all seven RSNs. Top: soft-voting ensemble of machine learning models using 30 pairwise distances of ICs' fALFF as input. Bottom: SVM-RBF using 50 features derived from pairwise distances of FD. Each model was evaluated using three accuracy measures: precision (TP/(TP + FP)), recall (TP/(TP + FN)), and F1 score ( $2 \times \text{precision} \times \text{recall} / (\text{precision} + \text{recall})$ ); support indicates the sample size of classes. The overall accuracy refers to the average accuracy over 10 iterations ± standard deviation.

Abbreviations: IC, independent component; RSN, resting-state network; fALFF, fractional amplitude of low-frequency fluctuation; PD-NC, PD with normal cognition; PD-MCI, PD with mild cognitive impairment; PDD, PD with dementia; SVM, support vector machine; FD, fractal dimension; TP, true positive; FP, false positive; FN, false negative.

(ie, Pdist), were then included as features in the multivariate ML models.

First, optimization procedures on the 595 pairwise Mahalanobis distances (Pdist) were applied, resulting in two distinct sets of features that yielded the highest classification accuracies for ML classifiers; namely 30 features for fALFF and 49 features for FD. These selected features represent indicators of the pairwise similarity between ICs, with one based on fALFF and the other on FD.

On conducting comprehensive analyses by employing various models and their combinations using soft- and hard-voting techniques, we found that the most accurate differentiation of PD-cognitive states (PD-NC, PD-MCI vs. PDD) was achieved by SVM classifiers when using FD-based features as input. FD classifiers demonstrated an average accuracy of  $78 \pm 1\%$  (weighted average precision: 0.80; recall: 0.80) (Table 2; Fig. 3B) over 10 iterations. Conversely, when employing fALFF-based features, we observed a lower overall accuracy of  $62.2 \pm 1.4\%$  (weighted average precision: 0.64; recall: 0.64) (Table 2; Fig. 3B) through soft-voting among NN, SVM, and RF models. When both features, fALFF and FD, were combined, the average accuracy reached  $76\% \pm 1.6\%$  with 44 input features. This suggests that this combination predominantly relied on FD features. We further delved into these results by conducting additional ML analyses on significant RSNs, as detailed in the Supporting Information.

Additionally, we provide a concise overview of some of the hyperparameters employed in our most successful SVM model using FD features. Table S5 provides comprehensive information on the pertinent FD features that contributed to the classification, and Table S6 presents the results of a model focused exclusively on the DMN, SMN, and CEN, achieving an overall accuracy of  $73.1\% \pm 1\%$ .

## Discussion

FD is progressively emerging in neurosciences as a method to detect the functional complexity of the neural system, thus possibly serving as an effective biomarker of disease progression.<sup>13,18,40</sup> To our knowledge, this is the first time that FD metric was applied to rs-fMRI data in PD population, with a particular focus on cognition. Here, we explored intrinsic brain activity neuronal dynamics at rest from two different perspectives: a linear method estimated using fALFF versus a nonlinear method using FD, in a large HC and PD cohort to identify differences across the entire PD-cognitive spectrum. ML models highlighted that FD—as an index of complexity of the neuronal dynamics of BOLD signal—was more accurate in differentiating among PD-cognitive states than fALFF, a more established metric to characterize the brain function at rest.

Our major finding is that PD patients present an increased neuronal dynamics complexity (estimated by FD) within the CEN and DMN, paralleled by a reduced spontaneous brain activity (estimated by fALFF) in these RSNs, compared to HC. Considering that a network is by definition a system with greater complexity, when it is highly specialized,<sup>27,41</sup> we can speculate that higher complexity within these RSNs possibly reflects brain network functional specialization, that is, local segregation.<sup>42,43</sup> Diverse dynamical reconfiguration of brain functional organization between segregated and integrated states associated with neurological disorders has been reported,<sup>42</sup> and this view is also supported by our previous study.<sup>6</sup> We demonstrated that PD is characterized by altered temporal properties in dynamic connectivity, with a longer dwell time in segregated states and a reduced number of transitions to the more integrated states, leading to increased local segregation and reduced “crosstalk” between brain networks, particularly in PDD.<sup>6</sup> Other studies have now confirmed our initial findings,<sup>44</sup> including a 5-year longitudinal study reporting increased functional brain disconnectivity with PD progression, that strongly correlated with global cognitive deterioration.<sup>45</sup>

Here, in line with these observations, PD-subgroup analyses show that the CEN and DMN neural dynamic complexity is strongly linked to cognitive status, because PDD presented a significant higher complexity in specific ICs—IC48 (CEN) and IC34 (DMN)—than PD-NC and PD-MCI, as well as in IC45 (DMN) compared to PD-NC, possibly suggesting an increased local segregation in these nodes associated with a more severe cognitive state. In addition, correlation analyses highlighted that greater complexity of neural dynamics within the IC45, located in the bilateral ACC as part of the DMN, was strongly associated to a worse cognitive performance in the memory domain as well as to disease severity (measured using the HY scale).

Notably, altered neuronal dynamics within the bilateral ACC supports the key role of this region in PD pathology, correlating with multiple PD nonmotor symptoms and being involved since the prodromal stage of the disease.<sup>46</sup> Indeed, ACC abnormalities (ie, functional and structural) have been associated with prodromal forms of subjective memory impairment,<sup>47</sup> but also to PD-MCI, showing a reduced thickness and white-matter alterations during the disease course.<sup>46,48</sup> ACC is commonly affected by both Lewy- and Alzheimer-type pathologies, thus identified as a regional PDD predictor in clinicopathological studies.<sup>49,50</sup> Overall, these observations suggest that greater complexity within these CEN nodes may be considered as a potential signature of PD-cognitive decline and progression. Monitoring the increased complexity of this critical hub located in the ACC (as part of the CEN) may be a new biomarker of PD phenotype linked to worse cognitive/

motor symptoms and thus increased daily-life disabilities. Further, longitudinal studies need to explore this assumption.

While considering the fALFF perspective within the CEN, a reduced spontaneous neuronal activity was observed in PD patients than HCs; further, PD-subgroup analyses showed that the reduced fALFF activity was linked to PD-cognitive deficits, as PDD patients presented a significant lower spontaneous neuronal activity than PD-NC in CEN, although no differences were noted with the PD-MCI group. Notably, these significant differences between PDD and PD-NC involved IC17 and IC25—located in the supramarginal gyrus and in the inferior/medial superior frontal gyrus, respectively. These results are consistent with previous evidence showing a reduced fALFF activity in PD patients compared to HCs in the frontal regions,<sup>3</sup> but not observed in PD-MCI versus PD-NC. Indeed, PDD was not included in their study design, preventing more in-depth analyses of more advanced PD-cognitive stages.<sup>3</sup> Therefore, our findings add to the view that a reduction in fALFF is associated with more severe PD-cognitive profiles.

However, it is worth considering that, unlike FD metrics, we did not find an association between fALFF activity and clinical/cognitive features within the CEN, despite the crucial role of this RSN in PD cognition.<sup>51</sup> This allows us to hypothesize that complexity indexes, such as FD, are more sensitive in capturing brain dynamics alterations associated with PD-cognitive severity rather than the standard linear metric, as fALFF.

Abnormal brain dynamics, characterized by increased complexity, were also present within the SMN in PD patients compared to HCs, although not paralleled by alterations in fALFF activity. Increased SMN complexity, possibly reflecting its increased segregation, supports the view of PD as a “disconnection syndrome,” characterized by increased FC within the SMN and reduced interactions with other brain modules.<sup>6,52</sup>

However, we did not find any difference in complexity across PD subgroups as well as no correlations with the clinical measures. Considering that SMN is sensitive to dopaminergic treatments, we can hypothesize that we failed to find an effect because PD patients were under medical treatment, and L-dopa may partially normalize the FC pattern, particularly within the SMN.<sup>53,54</sup> Further studies with drug-naïve or in “off medication” patients will be necessary to exclude potential L-dopa mitigating effects.

Another compelling result is that we observed an altered spontaneous neuronal activity also within the AN, where PD patients showed an increased fALFF activity compared to HCs, similar to previous evidence.<sup>55</sup> Notably, in this RSN, we did not observe a concomitant altered complexity index in PD, as measured using FD metrics. However, we found an opposed fALFF pattern when analyzing the differences between the PD

subgroups, with PDD showing a significant reduction in spontaneous neuronal activity in IC97 (AN) than PD-NC. This IC97 fALFF reduction, mostly located in the superior temporal gyrus, was closely associated with some clinical features. That is, a reduced IC97 neuronal activity was linked to a greater clinical severity (as assessed using MDS-UPDRS-III scores) and worse cognitive functioning—involving global cognition (MoCA), attention/working memory, and language abilities. Recent EEG evidence of a cohort of early PD with untreated hearing losses seems to support our findings,<sup>56</sup> as PD patients showed an altered neural processing (assessed by the auditory event-related potentials) compared to HCs, which was paralleled by a worse cognitive performance.<sup>56,57</sup> Therefore, aligned with this evidence, we can surmise that with disease progression, a functional reorganization of brain processes occurs, which is not necessarily more effective and can lead to detrimental effects on other processes, such as cognition. Indeed, it is not surprising that untreated hearing loss is more likely to exacerbate cognitive deficits, which are experienced by many PD patients during the progression of the disease.<sup>56</sup>

Therefore, we can surmise that the opposite (ie, increased) fALFF activity observed in the whole PD group than HCs was possibly a compensatory mechanism driven by patients in the early disease stages, which allocate more resources to auditory perceptual processing.<sup>56</sup>

Overall, these results emphasize that both metrics, fALFF and FD, are sensitive in detecting altered brain dynamics at rest in PD population; however, FD—as an index of BOLD complexity—may be more suitable to characterize brain dynamics abnormalities related to PD-cognitive decline than the more standard linear fALFF approach.

To further test the sensitivity of these metrics in predicting PD-cognitive states, ML models were run using as predictors the difference in complexity between ICs (by Mahalanobis distance), in terms of fALFF versus FD. We found that FD provided a higher accuracy of  $78 \pm 1\%$  that numerically outperformed the lower accuracy obtained using ML based on fALFF metric ( $62.2 \pm 1.4\%$ ). The best FD features mostly involved the CEN, DMN, SMN, and CB between-network connections and the CEN and DMN within-network connections (see Fig. 3B; Table S4).

A final consideration about our FD findings is that these only partially overlap, with previous evidence in the literature investigating other disorders/conditions using this metric on fMRI/EEG data. For instance, increased FD neural dynamics were associated to migraine severity and attack duration,<sup>18,40</sup> greater fatigue in multiple sclerosis,<sup>14</sup> disruption of cognitive control of pain,<sup>17</sup> and psychedelic drug assumptions.<sup>58</sup> By contrast, FD reductions have been linked to more severe disorders of consciousness,<sup>20</sup> worse cognitive functioning in AD patients,<sup>13</sup> and more severe

structural damage in acute stroke.<sup>16</sup> This heterogeneity among previous reports is not surprising, considering that dynamic reconfiguration of brain FC can vary based on the investigated neurological disorder following different reconfigurations in both normal aging and neurodegenerative conditions.<sup>42</sup> Different underlying mechanisms and brain network reorganization characterize PD-cognitive decline. A strength of our findings is that increased neural dynamic complexity in PD is confirmed by altered fALFF activity and by the relationship with clinical/cognitive PD features, possibly supporting our hypothesis that greater complexity can be an index of increased RSN segregation.<sup>24</sup>

There are a few limitations that should be considered in the interpretation of our results. First, all patients were studied after the intake of L-dopa therapy in their best medical condition at the time of MRI, which was crucial to reduce discomfort and motion artifacts as well as limit variability in FC related to medication effect. We acknowledge we did not measure peripheral L-dopa plasma levels at the time of MRI, but similar to other studies we based our assumption of efficacy on verification of “on medication” motor status in each patient.<sup>59</sup> Second, we acknowledge our data were obtained using a 1.5-T MRI scanner, although other previous studies adopted the same approaches (fALFF and FD) using MRI scanners with the same field strength.<sup>60,61</sup> Finally, previous evidence using ML approaches based their predictions mostly on motor severity,<sup>62</sup> whereas here we focused on cognitive decline, which is one of the most important L-dopa nonresponsive features in PD.<sup>63</sup> ■

**Acknowledgments:** We thank all patients, their families, and caregivers for participating in this study. We acknowledge cofunding from Next Generation EU, in the context of the National Recovery and Resilience Plan, Investment PE8—Project Age-It: “Ageing Well in an Ageing Society.” This resource was cofinanced by the Next Generation EU (Decreto Ministeriale (DM) 1557 11 October 2022). The views and opinions expressed are only those of the authors and do not necessarily reflect those of the European Union or the European Commission. Neither the European Union nor the European Commission can be held responsible for them.

## Data Availability Statement

The data that support the findings of this study are available on request from the corresponding author. The data are not publicly available due to privacy or ethical restrictions.

## References

1. Bloem BR, Okun MS, Klein C. Parkinson's disease. *Lancet* 2021; 397:2284–2303.
2. Antonini A, Bravi D, Sandre M, Bubacco L. Immunization therapies for Parkinson's disease: state of the art and considerations for future clinical trials. *Expert Opin Investig Drugs* 2020;29:685–695.
3. Rong S, Zhang P, He C, et al. Abnormal neural activity in different frequency bands in Parkinson's disease with mild cognitive impairment. *Front Aging Neurosci* 2021;13:709998.

4. Wang X, Wei W, Bai Y, et al. Intrinsic brain activity alterations in patients with Parkinson's disease. *Neurosci Lett Epub* 2023;809:137298.
5. Wolters AF, van de Weijer SCF, Leentjens AFG, Duits AA, Jacobs HIL, Kuijff ML. Resting-state fMRI in Parkinson's disease patients with cognitive impairment: a meta-analysis. *Parkinsonism Relat Disord* 2019;62:16–27.
6. Fiorenzato E, Strafella AP, Kim J, et al. Dynamic functional connectivity changes associated with dementia in Parkinson's disease. *Brain* 2019;142:2860–2872.
7. Kehagia AA, Barker RA, Robbins TW. Neuropsychological and clinical heterogeneity of cognitive impairment and dementia in patients with Parkinson's disease. *Lancet Neurol* 2010;9:1200–1213.
8. Porcaro C, Mayhew SD, Marino M, Mantini D, Bagshaw AP. Characterisation of Haemodynamic activity in resting state networks by fractal analysis. *Int J Neural Syst* 2020;30:2050061.
9. Kesić S, Spasić SZ. Application of Higuchi's fractal dimension from basic to clinical neurophysiology: a review. *Comput Methods Programs Biomed* 2016;133:55–70.
10. Naik GR, Arjunan S, Kumar D. Applications of ICA and fractal dimension in sEMG signal processing for subtle movement analysis: a review. *Australas Phys Eng Sci Med* 2011;34:179–193.
11. Ziukelis ET, Mak E, Dounavi M-E, Su L, T O'Brien J. Fractal dimension of the brain in neurodegenerative disease and dementia: a systematic review. *Ageing Res Rev* 2022;79:101651.
12. Al-Nuaimi AH, Jammeh E, Sun L, Ifeachor E. Higuchi fractal dimension of the electroencephalogram as a biomarker for early detection of Alzheimer's disease. *Annu Int Conf IEEE Eng Med Biol Soc* 2017;2017:2320–2324.
13. Smits FM, Porcaro C, Cottone C, Cancelli A, Rossini PM, Tecchio F. Electroencephalographic fractal dimension in healthy ageing and Alzheimer's disease. *Plos One* 2016;11:e0149587.
14. Porcaro C, Cottone C, Cancelli A, Rossini PM, Zito G, Tecchio F. Cortical neurodynamics changes mediate the efficacy of a personalized neuromodulation against multiple sclerosis fatigue. *Sci Rep* 2019;9:18213.
15. Sheelakumari R, Rajagopalan V, Chandran A, et al. Quantitative analysis of grey matter degeneration in FTD patients using fractal dimension analysis. *Brain Imaging Behav* 2018;12:1221–1228.
16. Zappasodi F, Olejarczyk E, Marzetti L, Assenza G, Pizzella V, Tecchio F. Fractal dimension of EEG activity senses neuronal impairment in acute stroke. *Plos One* 2014;9:e100199.
17. Porcaro C, Di Renzo A, Tinelli E, et al. Haemodynamic activity characterization of resting state networks by fractal analysis and thalamocortical morphofunctional integrity in chronic migraine. *J Headache Pain* 2020;21:112.
18. Porcaro C, Di Renzo A, Tinelli E, et al. Hypothalamic structural integrity and temporal complexity of cortical information processing at rest in migraine without aura patients between attacks. *Sci Rep* 2021;11:18701.
19. Porcaro C, Marino M, Carozzo S, et al. Fractal dimension feature as a signature of severity in disorders of consciousness: an EEG study. *Int J Neur Syst* 2022;32:2250031.
20. Varley TF, Craig M, Adapa R, et al. Fractal dimension of cortical functional connectivity networks & severity of disorders of consciousness. *Plos One* 2020;15:e0223812.
21. Borri A, Cerasa A, Tonin P, Citrigno L, Porcaro C. Characterizing fractal genetic variation in the human genome from the Hapmap project. *Int J Neural Syst* 2022;32:2250028.
22. Postuma RB, Berg D, Stern M, et al. MDS clinical diagnostic criteria for Parkinson's disease. *Mov Disord* 2015;30:1591–1601.
23. Jost ST, Kaldenbach M-A, Antonini A, et al. Levodopa dose equivalency in Parkinson's disease: updated systematic review and proposals. *Mov Disord* 2023;38:1236–1252.
24. Fiorenzato E, Antonini A, Camparini V, Weis L, Semenza C, Biundo R. Characteristics and progression of cognitive deficits in progressive supranuclear palsy vs. multiple system atrophy and Parkinson's disease. *J Neural Transm (Vienna)* 2019;126:1437–1445.
25. Allen EA, Damaraju E, Plis SM, Erhardt EB, Eichele T, Calhoun VD. Tracking whole-brain connectivity dynamics in the resting state. *Cereb Cortex* 2014;24:663–676.
26. Zou Q-H, Zhu C-Z, Yang Y, et al. An improved approach to detection of amplitude of low-frequency fluctuation (ALFF) for resting-state fMRI: fractional ALFF. *J Neurosci Methods* 2008;172:137–141.
27. Marino M, Liu Q, Samogin J, et al. Neuronal dynamics enable the functional differentiation of resting state networks in the human brain. *Hum Brain Mapp* 2019;40:1445–1457.
28. Di Ieva A, Grizzi F, Jelinek H, Pellionisz AJ, Losa GA. Fractals in the neurosciences, part I: general principles and basic neurosciences. *Neuroscientist* 2014;20:403–417.
29. Di Ieva A. The fractal geometry of the brain. *Fractal geometry and nonlinear. Anal in Med and Biol* 2016;2:1.
30. Raghavendra BS, Dutt DN. Signal characterization using fractal dimension. *Fractals* 2010;18:287–292.
31. Higuchi T. Approach to an irregular time series on the basis of the fractal theory. *Phys D: Nonlinear Phenom* 1988;31:277–283.
32. Katz MJ. Fractals and the analysis of waveforms. *Comput Biol Med* 1988;18:145–156.
33. Esteller R, Vachtsevanos G, Echaz J, Litt B. A comparison of waveform fractal dimension algorithms. *IEEE Trans Circuits Sys I: Fund Theor Appl* 2001;48:177–183.
34. Mahadevan AS, Tooley UA, Bertolero MA, Mackey AP, Bassett DS. Evaluating the sensitivity of functional connectivity measures to motion artifact in resting-state fMRI data. *Neuroimage* 2021;241:118408.
35. Geerligs L, Cam-CAN HRN. Functional connectivity and structural covariance between regions of interest can be measured more accurately using multivariate distance correlation. *Neuroimage* 2016;135:16–31.
36. Yoo K, Rosenberg MD, Noble S, Scheinost D, Constable RT, Chun MM. Multivariate approaches improve the reliability and validity of functional connectivity and prediction of individual behaviors. *Neuroimage* 2019;197:212–223.
37. Ferracuti F, Iarlori S, Mansour Z, Monteriù A, Porcaro C. Comparing between different sets of preprocessing, classifiers, and channels selection techniques to optimise motor imagery pattern classification system from EEG pattern recognition. *Brain Sci* 2022;12:57.
38. Peng H, Long F, Ding C. Feature selection based on mutual information criteria of max-dependency, max-relevance, and min-redundancy. *IEEE Trans Pattern Anal Mach Intell* 2005;27:1226–1238.
39. Allen EA, Erhardt EB, Damaraju E, et al. A baseline for the multivariate comparison of resting-state networks. *Front Syst Neurosci* 2011;5:2.
40. Porcaro C, Di Renzo A, Tinelli E, et al. A hypothalamic mechanism regulates the duration of a migraine attack: insights from microstructural and temporal complexity of cortical functional networks analysis. *Int J Mol Sci* 2022;23:13238.
41. Tononi G, Sporns O, Edelman GM. A measure for brain complexity: relating functional segregation and integration in the nervous system. *Proc Natl Acad Sci* 1994;91:5033–5037.
42. Wang R, Liu M, Cheng X, Wu Y, Hildebrandt A, Zhou C. Segregation, integration, and balance of large-scale resting brain networks configure different cognitive abilities. *Proc Natl Acad Sci U S A* 2021;118:e2022288118.
43. Wig GS. Segregated systems of human brain networks. *Trends Cogn Sci* 2017;21:981–996.
44. Cao Y, Si Q, Tong R, Zhang X, Li C, Mao S. Abnormal dynamic functional connectivity changes correlated with non-motor symptoms of Parkinson's disease. *Front Neurosci* 2023;17:1116111.
45. Yassine S, Gschwandtner U, Auffret M, et al. Functional brain dysconnectivity in Parkinson's disease: a 5-year longitudinal study. *Mov Disord* 2022;37:1444–1453.
46. Vogt BA. Cingulate cortex in Parkinson's disease. In: Vogt BA, ed. *Handbook of Clinical Neurology*. London: Elsevier; 2019: 253–266.
47. Song I-U, Kim J-S, Chung S-W, Lee K-S, Oh J-K, Chung Y-A. Early detection of subjective memory impairment in Parkinson's disease using cerebral perfusion SPECT. *Biomed Mater Eng* 2014;24: 3405–3410.

48. Gao Y, Nie K, Huang B, et al. Changes of brain structure in Parkinson's disease patients with mild cognitive impairment analyzed via VBM technology. *Neurosci Lett* 2017;658:121–132.
49. Compta Y, Pereira JB, Ríos J, et al. Combined dementia-risk biomarkers in Parkinson's disease: a prospective longitudinal study. *Parkinsonism Relat Disord* 2013;19:717–724.
50. Kövari E, Gold G, Herrmann FR, et al. Lewy body densities in the entorhinal and anterior cingulate cortex predict cognitive deficits in Parkinson's disease. *Acta Neuropathol* 2003;106:83–88.
51. Tessitore A, Cirillo M, De Micco R. Functional connectivity signatures of Parkinson's disease. *J Parkinson's Dis* 2019;9:637–652.
52. Göttlich M, Münte TF, Heldmann M, Kasten M, Hagenah J, Krämer UM. Altered resting state brain networks in Parkinson's disease. *Plos One* 2013;8:e77336.
53. Caspers J, Rubbert C, Eickhoff SB, et al. Within- and across-network alterations of the sensorimotor network in Parkinson's disease. *Neuroradiology* 2021;63:2073–2085.
54. Esposito F, Tessitore A, Giordano A, et al. Rhythm-specific modulation of the sensorimotor network in drug-naïve patients with Parkinson's disease by levodopa. *Brain* 2013;136:710–725.
55. Zhang P, Gao Y, Hu Y, et al. Altered fractional amplitude of low-frequency fluctuation in anxious Parkinson's disease. *Brain Sci* 2023; 13:87.
56. Folmer RL, Vachhani JJ, Riggins A. Electrophysiological evidence of auditory and cognitive processing deficits in Parkinson disease. *Biomed Res Int* 2021;2021:6610908.
57. Lin FR, Metter EJ, O'Brien RJ, Resnick SM, Zonderman AB, Ferrucci L. Hearing loss and incident dementia. *Arch Neurol* 2011;68:214–220.
58. Varley TF, Carhart-Harris R, Roseman L, Menon DK, Stamatakis EA. Serotonergic psychedelics LSD & psilocybin increase the fractal dimension of cortical brain activity in spatial and temporal domains. *Neuroimage* 2020;220:117049.
59. Poewe W, Antonini A, Zijlmans JC, Burkhard PR, Vingerhoets F. Levodopa in the treatment of Parkinson's disease: an old drug still going strong. *CIA* 2010;5:229–238.
60. Jao C-W, Soong B-W, Wang T-Y, et al. Intra- and inter-modular connectivity alterations in the brain structural network of spinocerebellar ataxia type 3. *Entropy* 2019;21:317.
61. Sokunbi MO, Gradin VB, Waiter GD, et al. Nonlinear complexity analysis of brain fMRI signals in schizophrenia. *Plos One* 2014;9: e95146.
62. Nguyen KP, Raval V, Treacher A, et al. Predicting Parkinson's disease trajectory using clinical and neuroimaging baseline measures. *Parkinsonism Relat Disord* 2021;85:44–51.
63. Antonini A, Emmi A, Campagnolo M. Beyond the dopaminergic system: lessons learned from levodopa resistant symptoms in Parkinson's disease. *Mov Disord Clin Pract* 2023;10:S50–S55.

## Supporting Data

Additional Supporting Information may be found in the online version of this article at the publisher's web-site.